ORIGINAL PAPER

Density functional theory and molecular dynamics investigations on substituted banana-shaped compounds

**Ananda Rama Krishnan Selvaraj ·
Wolfgang Weissflog · Rudolf Friedemann**

Abstract Density functional theory (DFT) calculations and molecular dynamics (MD) simulations on the atomic level were performed on three different substituted banana-shaped compounds derived from 1,3-phenylene bis[4-(4-n-hexyloxyphenyliminomethyl)benzoate] (P-6-O-PIMB). The DFT studies were carried out on the isolated molecules, and in the MD simulations clusters were treated with up to 64 monomers. The effect of polar substituents, such as chlorine and the nitro group, on the central 1,3-phenylene unit of banana-shaped compounds was investigated. In particular, flexibility, polarity, electrostatic potential (ESP) group charge distributions, B-factors, bending angles and molecular lengths were considered. The MD results were analysed by trajectories of significant torsion angles as well as order parameters such as radial atom pair distribution functions g(r), orientational correlation functions g(o), diffusion coefficients (D) and root mean square deviations (RMSD) values. The g(r) and g(o) values show that a certain long range order is generated by the introduction of a NO_2 group in the 2-position of the central 1,3-phenylene ring. In contrast, the chlorination at the 4 and 6 positions of

the central 1,3-phenylene unit decreases the long range order tendency by its perturbation effect on the conformations in such molecules. Moreover, g(r) and g(o) values, as well as diffusion coefficients, show that in the NO_2 substituted compound the formation of microphase areas is preferred. Finally, the aggregation effect in such compounds was studied in a systematic way by a comparison of the conformational properties of the isolated molecules and the monomers in the clusters.

Keywords Banana-shaped molecules · Bending angle · Order parameters · Diffusion coefficients

Introduction

Banana-shaped or bent-core liquid crystals have become a new dimension in the field of liquid crystallography since the significant research work of T. Niori et al. [1]. The special interest of such compounds lies in their various application-oriented properties such as ferroelectrics, anti-ferroelectrics, non-linear optical aspects and the formation of chiral mesophases from achiral molecules. The characteristic feature of such molecules is their bent shape, which allows them to be arranged in a regular manner in smectic layers. The tight packing of the bent cores leads to a long-range correlation of the lateral dipoles and the macroscopic polar order in the smectic layers [2]. Review articles on this type of molecule illustrate their importance and the peculiar interest in the mesophases formed by such compounds [3–6]. Banana-shaped liquid crystals have gained their special name in the mesophase nomenclature because of their so-called "B phases" (B1–B8). If the phase structure is sufficiently known, the name smectic, or columnar, phase together with related indices such as polar, synclinic,

A. R. K. Selvaraj · R. Friedemann (✉)
Institut für Chemie / Organische Chemie,
Martin-Luther-Universität Halle-Wittenberg,
Kurt-Mothes-Strasse 2,
06120 Halle (Saale), Germany
e-mail: rudolf.friedemann@chemie.uni-halle.de

W. Weissflog
Institut für Chemie /Physikalische Chemie,
Martin-Luther-Universität Halle-Wittenberg,
Mühlpforte 1,
06108 Halle (Saale), Germany

anticlinic, antiferroelectric and ferroelectric should be preferred. The influence of polar substituents in such compounds is more significant than in rod-like mesogenic molecules [7–15], as indicated by strong effects on the clearing temperature, mesomorphism and directional properties such as dielectric anisotropy. Substitution on banana-shaped molecules can be divided into modifications to the central unit or to the rings of the legs—in each case the effect on the mesophase behaviour is clearly different. Theoretical investigations based on the conformational, polar and aggregation properties of banana-shaped compounds have been limited to date [16–23]. Simulations on such systems were carried out mostly within Monte Carlo techniques including global patterns for the shape and the polarity of the molecules [24–34]. Recently, molecular dynamics (MD) simulations using the program AMBER were made for an isolated molecule of compound *2* (see Table 2) on a water surface [35]. In our work, systematic theoretical investigations were performed with the aim of studying the effect of polar substitutions at the central 1,3-phenylene unit on the conformational properties and aggregation behaviour of banana-shaped molecules. The conformational properties of the molecules were investigated by density functional theory (DFT) calculations and MD simulations. In recent years, the MD method has been developed as an appropriate technique to study the dynamics and the aggregation behaviour of larger molecules [36–39]. MD simulations on the atomic level have been carried out on banana-shaped compounds to study the influence of substitution on conformational properties and aggregation effects both in the isolated molecule and in clusters with up to 64 monomers. Three different banana-shaped compounds of the 1,3-phenylene bis [4-(4-n-alkyloxyphenyliminomethyl) benzoate] (P-6-O-PIMB) type were considered. The main structure, and the definition of the systems together with their mesophase properties, are shown in Fig. 1 and Table 1. It is remarkable that the unsubstituted compound (*1*), the chlorinated

Table 1 Notation of the systems and their mesophase behaviour. *CT* Clearing temperature

Number	R_2	R_4	R_6	Mesophase sequence[a]	CT[b]
(*1*)	H	H	H	B4 143.6 B3 159 B1 173 I[c]	173 [3]
(*2*)	H	Cl	Cl	Cr 127 N 165 I	165 [3]
(*3*)	NO_2	H	H	Cr 107 B7 177 I	177 [3]

[a] Transition temperature in parentheses in °C
[b] CT in °C
[c] On cooling

compound (*2*) and the derivative with a nitro group (*3*) show significantly different mesogenic properties.

The conformational flexibility of the wings was calculated from relaxed rotational barriers as well as from trajectories related to the torsion angle ϕ_1. For banana-shaped molecules, the bending angle γ is a relevant structural parameter. A simple model for the calculation of γ was used [21]. The global polarity of the considered banana-shaped molecules can be obtained from calculations of the dipole moment, μ, and the polarisability, α, as well as the electron density, ρ. Therefore, the influence of substituents on these quantities was calculated. The effect of substitution on the aggregation behaviour of such compounds was investigated by MD studies on clusters. The MD results were analysed by trajectories of significant torsion angles as well as structural parameters like B-factor values of connecting group atoms, bending angles and molecular lengths. The structure formation, order effects and mobility in the clusters were illustrated by radial atom pair distribution functions [g(r)], orientational correlation functions [g(o)], diffusion coefficients (D), and root mean square deviation (RMSD) values. Moreover, an essential aim of this work was the calculation of significant structural properties for both the isolated molecule and the monomers in the clusters to gain some hints as to the aggregation effects of substituted banana-shaped compounds.

Computational details

Density functional theory calculations on the B3LYP/6-31G (d) level were performed using the program package Gaussian98 [40]. The relaxed rotational barriers were generated with respect to the torsion angle ϕ_1 (see Fig. 2) by a partial optimisation procedure. The dipole moment and its components, as well as the diagonal elements of the polarisability, were calculated for the most stable conformations and their dependency with respect to torsion angle ϕ_1 was analysed. The bending angle γ was calculated both
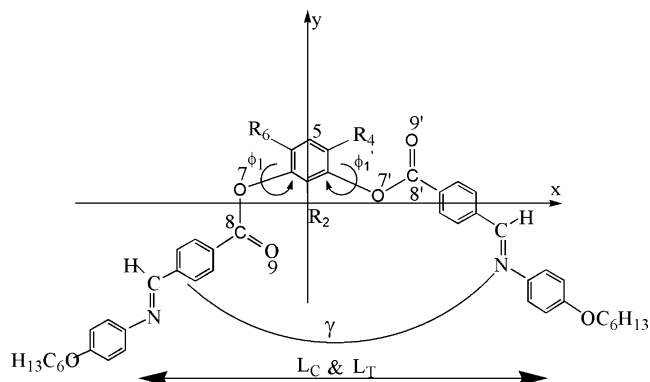

Fig. 1 Definition of banana-shaped systems with significant torsion angles (ϕ_1, ϕ_1'), reference coordinate system, bending angle (γ) and molecular lengths (L_C core and L_T total length)

within the DFT and MD methods using a model illustrated in a recent paper [21]. A simple procedure was used for the calculation of a global pattern of charge along the legs of the molecule. The atomic net charges of a molecule were calculated from the fit to reproduce its electrostatic potential (ESP) charges. For the phenyl rings, the ESP group charges are defined by summarising the charges of the corresponding carbon atoms and localising the values at the centres of the rings. In this way, the ESP group charges and their positions are comparable for the most stable conformations of the five-ring mesogens of the 1,3-phenylene type.

Moreover, MD simulations were carried out, implementing AMBER7 version using a GAFF force field [41, 42]. Atomic net charges for the molecules were adapted from the fit to reproduce the electrostatic potential within the HF/6-31G(d) level. The procedure is consistent with the defined atomic charges for amino acid fragments in the AMBER program [43]. Classical MD simulations were performed on isolated molecules under vacuum at 300 K and their clearing temperatures (CTs) and a simulation time of 1 ns. A time step of 0.5 fs was used in all simulations and the non-bonded interactions were calculated with a cut-off radius of 10,000 pm. The MD simulations on the clusters were performed with 64 monomers using an antiferroelectric starting structure model [2] for all systems. For the treatment of the clusters a total simulation time of 3 ns and a time step of 0.5 fs were used at two different temperatures including heating phases. Equilibration phases of 1 ns were taken into account for the analysis of the MD data both at 300 K and at the CT. The MD simulations were carried out with constant pressure (n, p, T) conditions. The SHAKE algorithm [44] was used only for hydrogen atoms. The non-bonded interactions in the clusters were calculated with a cut-off radius of 1,000 pm. The MD results were analysed by a graphics tool developed in our group at an Octane workstation and already utilised for mesogenic and biochemical systems [45, 46], and the AMBER7 standard tool for MD analyses, PTRAJ. From the MD results the trajectory of the torsion angle ϕ_1 was calculated. The B-factor value for the connecting group atoms was considered as a good indicator of the conformational flexibility and thermal motion of the molecules [47]. The connecting groups have a major influence on the flexibility and polarity of banana-shaped molecules. Therefore, the B-factor values were calculated for connecting group atoms. The histograms for the bending angle distribution were analysed. From the full width at half maximum (FWHM) values of the bending angle, its range can be evaluated. The molecular length was considered as core length (L_C)—the distance between oxygen atoms of the hexyloxy groups—and total length (L_T)—the distance between the terminal carbon atoms of the hexyloxy chains. The structure formation in the clusters can be analysed by the calculation of radial atom pair distribution function by g(r) [48]. The g(r) values were related to the reference atom C2 of the central ring. Further information on the arrangement of the molecules in the cluster can be estimated from evaluation of the orientation correlation function g(o). The g(o) data are obtained from the calculation of the radial dependence of the absolute cosines between the vectors of the reference atoms C2 and C5, which determine the orientation of the central rings in the cluster. Hints on the mobility of the molecules in the cluster can be achieved from the calculation of the diffusion coefficients D using the Einstein model within the MD procedure [49–51].

Results

DFT results

Relaxed rotational barriers

The relaxed rotational barriers of the significant torsion angle ϕ_1 indicate that the conformational flexibility of the legs of the banana-shaped molecules is essentially determined by the position of the polar substituents at the central unit. This is illustrated in Fig. 2.

The system (1) shows a high flexibility of the legs over the whole range of ϕ_1 with barriers lower than 10 kJ mol^{-1}. The substituted molecules indicate a different conformational behaviour. The substitution of a nitro group at the 2-position (3) causes energetically unfavoured conformations only for the range $-30° < \phi_1 < 30°$. The relative energies of the other areas are lower than 10 kJ mol^{-1}. Obviously, the nitro group substitution in the 2-position perturbs the conformational degree of freedom on the legs of these compounds in a limited way only. However, chlorine
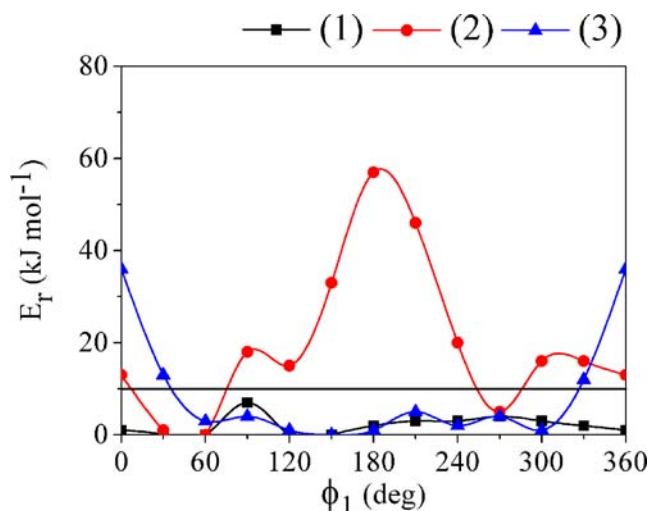
Fig. 2 Relaxed rotational barriers [density functional theory (DFT)] related to the torsion angle ϕ_1 for systems (1), (2) and (3)

substitutions in 4- and 6-positions (2) essentially decrease the flexibility of the legs in such molecules, resulting in a relaxed rotational barrier of about 60 kJ mol^{-1} and small areas for preferred conformers (E_r<10 kJ mol^{-1}). The different flexibility of the legs in these banana-shaped molecules can also influence their aggregation behaviour.

Dipole moments, polarisabilities, bending angles and ESP group charges

The dependency of the dipole moment (μ), polarisability (α) and the bending angle (γ) with constraints to the torsion angle ϕ_1 for the three systems is shown in Fig. 3. The one-fold scans of the dipole moments related to the torsion angle ϕ_1 indicate a larger range (4–6 Debye) for systems (1) and (2) but a lower range (2–4 Debye) for system (3). The energy weighted dipole moments including conformations with a relative energy lower than 10 kJ mol^{-1} show the sequence (1): 4.51 D >(2): 3.83 D > (3): 3.24 D.

For completeness, the dipole moments and their components of the most stable conformations of the three molecules are given in Table 2. In all three systems the main contribution to μ comes from the μ_y component.

From the diagonal elements of the polarisability (see Table 2) it follows that α_{XX} is the essential component that is oriented to the long axis of the molecule. The dependence of α_{XX} related to ϕ_1 is illustrated in Fig. 3. The trends in the curves confirm the sequence of α_{XX} for the most stable conformers α_{XX} (3)<α_{XX} (1)<α_{XX} (2) (Table 2). These findings are supported by the energy-weighted values α_{XX} including conformations lower than 10 kJ mol^{-1} α_{XX}(3) 1036<α_{XX}(1) 1059<α_{XX}(2) 1108.

The α_{XX} values of the most stable conformers correlate with the core (L_C) but not with the total (L_T) lengths (Table 2). The one-fold scan of the bending angle γ related to the torsion angle ϕ_1 is given in Fig. 3. In some way, the curves of the dependency of γ are comparable with those of α_{XX} for the corresponding systems. Moreover, from the electrostatic potential group charges (q/ESP), a global pattern of the charge distribution at the aromatic rings of the molecules can be calculated. The q/ESP values for the systems at the centres of the aromatic rings are illustrated in Fig. 4.

The charges at the connecting groups show no significant changes for the systems that are not drawn in Fig. 4 for reasons of clarity. The electron density ρ (ρ corresponds to -q/ESP) on the central ring A, and on the external rings C, C′, of the compounds correlates with the mesophase properties of the three banana-shaped compounds considered. In cases where the electron density on the central ring is higher than, or comparable to, that of the external rings ρ(A) ≥ ρ(C, C′), a B-phase formation like that in systems (1) and (3) is observed. In the opposite case, i.e. ρ(A) < ρ(C, C′), no B-phases are observed [system (2)]. As in similar
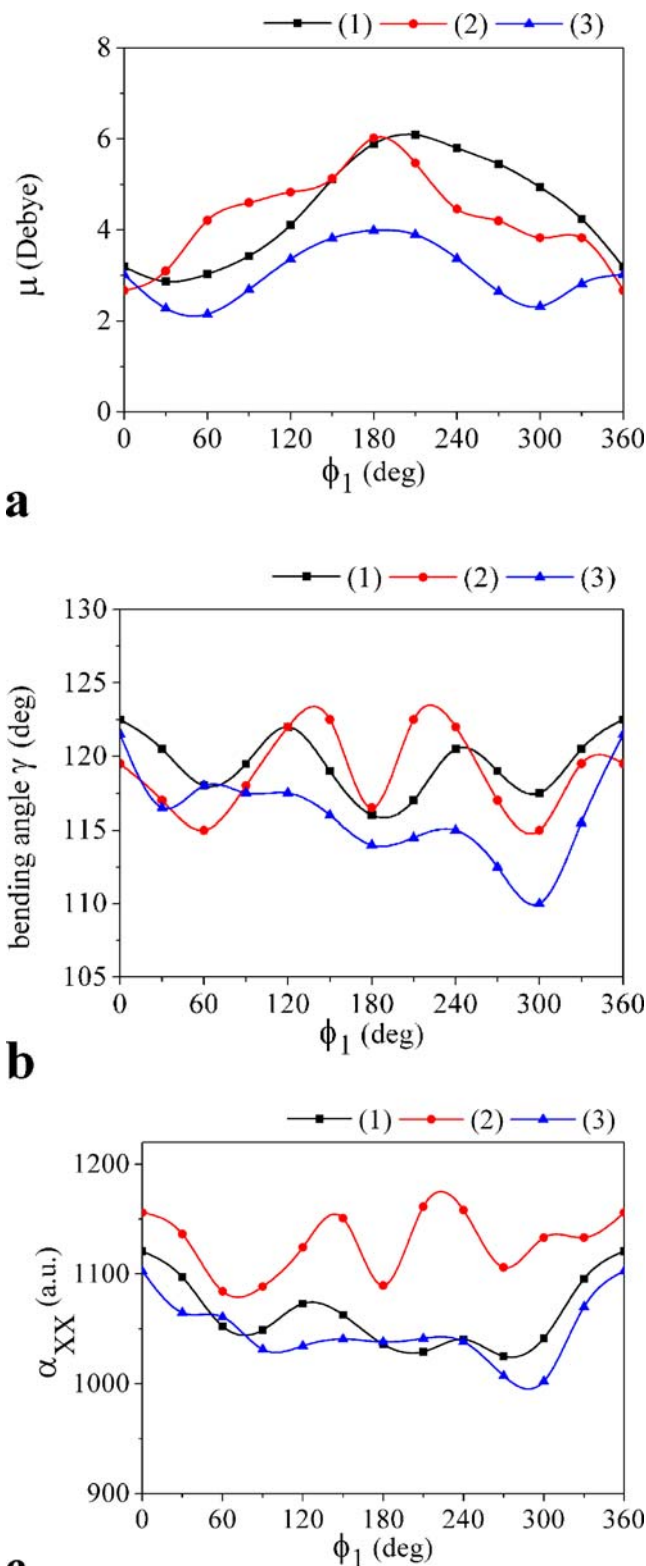

Fig. 3 a-c One-fold scans (DFT) related to the torsion angle ϕ_1. **a** Dipole moments μ, **b** bending angles γ, **c** diagonal components α_{xx} of the polarisability

Table 2 Dipole moments (μ, in Debye) and their components, diagonal elements α_{xx} of the polarisability (in a.u.; 1 a.u. is approximately 1.649 10^{-41} C^2 m^2 J^{-1}), bending angle γ (degrees), and values for the molecular lengths (L_C core and L_T total length, Å) of the most stable conformations of the three systems

System	μ_x	μ_y	μ_z	μ	α_{XX}	α_{YY}	α_{ZZ}	γ	L_T	L_T
(1)	−0.05	−4.75	−0.09	4.76	1064	606	305	120	26.12	40.06
(2)	0.46	−4.07	−0.60	4.14	1085	623	361	115	26.77	38.45
(3)	−0.09	−3.77	0.03	3.77	1029	670	345	116	25.37	37.64

types of five-ring banana-shaped systems the global pattern of charge distribution on the centres of the rings along the legs shows an alternating behaviour [52]. Significant changes in the electron density on the rings in homologous series of banana-shaped systems hint at for different phase properties.

MD results

Trajectories of torsion angle ϕ_1

MD simulations were performed on the isolated molecules in vacuum at 300 K and at the clearing temperatures of the compounds. The trajectories of the torsion angle ϕ_1 for the three systems at 300 K are shown in Fig. 5. The MD results on isolated molecules support the conformational findings from the relaxed rotational barriers within the DFT method (Fig. 2). From the trajectories of the torsion angle ϕ_1, the sequence for the flexibility of the legs (1)>(3)>(2) can be concluded. The corresponding trajectories at the clearing temperature of the compounds that are not shown indicate a similar trend. The flexibility of the legs is increased in all cases by the higher temperature but the main differences in the conformational behaviour of the molecules are retained.

In order to investigate the flexibility of the legs in the banana-shaped molecules in the aggregate state, MD simulations on clusters with 64 monomers were performed. The MD results on clusters revealed similar trajectories of ϕ_1 for a molecule in the environment of the other molecules generated at 300 K and at the clearing temperature of the compounds (Fig. 6).

It is remarkable that the conformational degree of freedom for the legs of the banana-shaped molecules in the clusters is significantly reduced in all systems. Obviously, the environment of the other molecules leads in all cases to the effect that only small areas of ϕ_1 are preferred but the values are different for the different systems. The results are in agreement with the findings of Samulski on the reduced conformational flexibility of aliphatic chains in the condensed state, which is known as the "cage effect" [53]. This means that, also in the clusters, substitution of the molecules leads to essentially different preferred arrangements of the cores. The corresponding trajectories at the clearing temperature of the compounds

are not illustrated but show the same trends. The temperature effect causes a certain broadening of the areas of ϕ_1. Comparison of the trajectories of isolated molecules (Fig. 5) and the corresponding trajectories of molecules in the cluster environment (Fig. 6) indicates a large aggregation effect regarding the conformational behaviour of the banana-shaped mesogens.

B-factors

B-factors can be used as a measure to describe the mobility of groups or atoms during the MD run [46]. In the investigated systems the B-factors (8/3 $\pi^2<\Delta r^2>$) of the carbonyl oxygen atoms of the ester linkage groups can serve as an indicator for the mobility of the legs of the banana-shaped systems. Therefore, the B-factors are calculated for a molecule in vacuum and in the cluster environment both at 300 K and at the clearing temperature. The values for a molecule in the cluster environment are illustrated in Fig. 7.

A considerable temperature effect on the B-factors was found. In the cluster environment, the B-factors are higher at the clearing temperature than at 300 K. The largest effect was obtained for system (2). For the isolated molecules in vacuum, the corresponding B-factors are generally higher up to 60 $Å^2$ but there is no notable temperature effect in the values. In all systems the values of the B-factor were
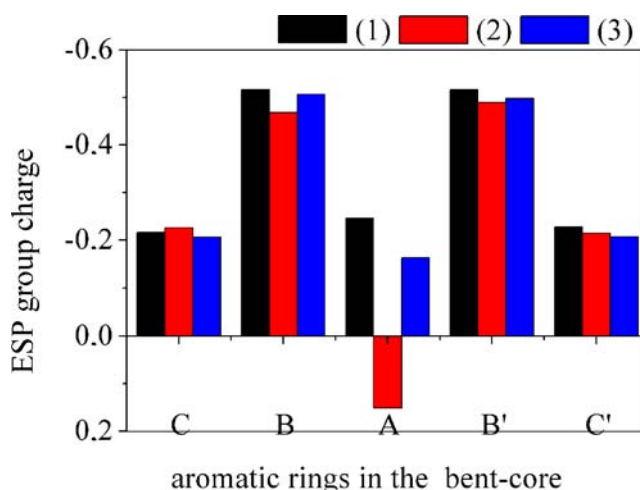
Fig. 4 Electrostatic potential group charges (q/ESP) on the centres of the rings for three systems
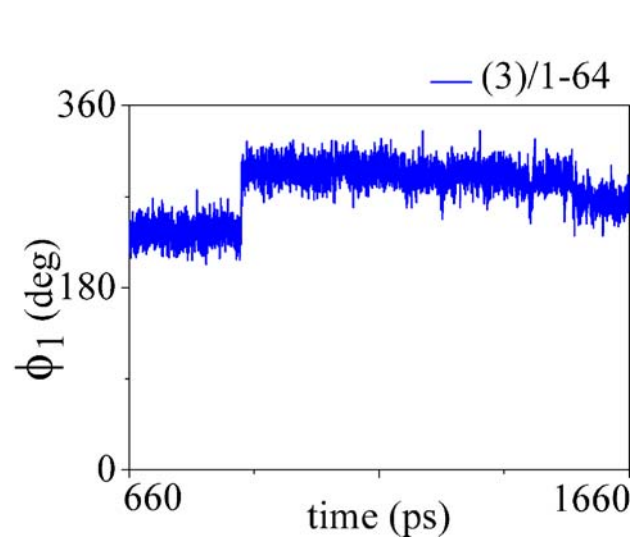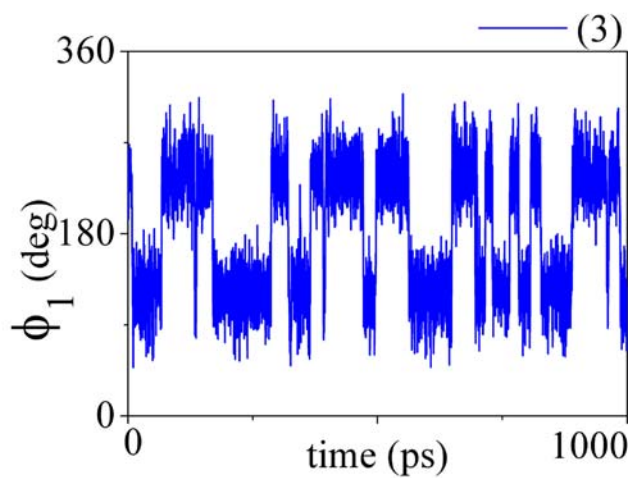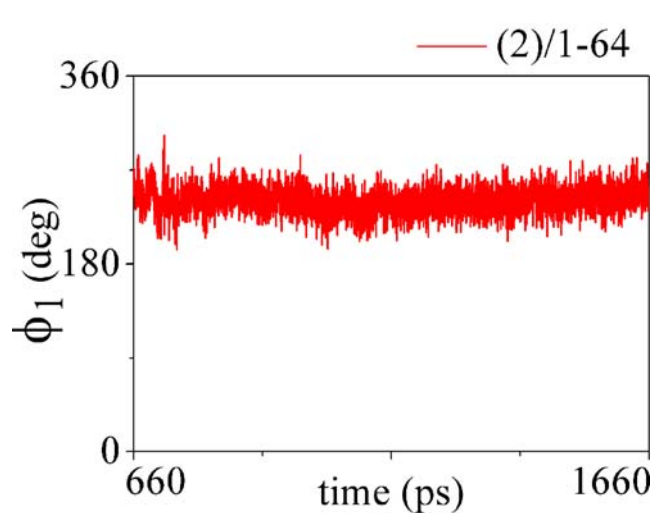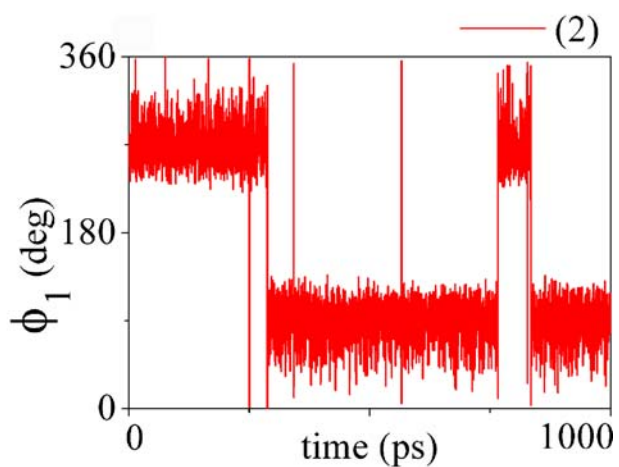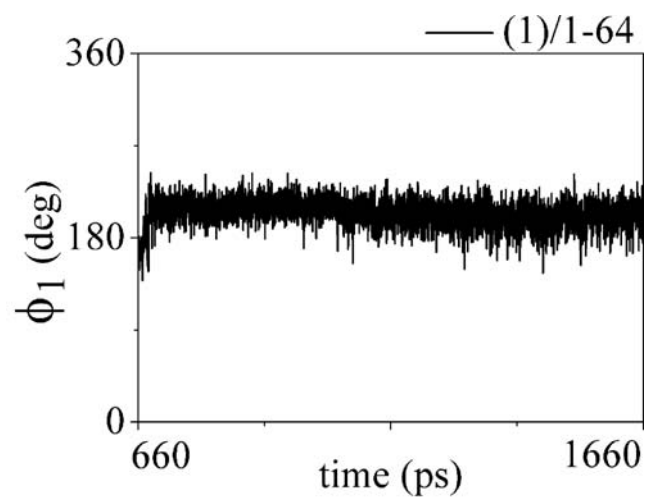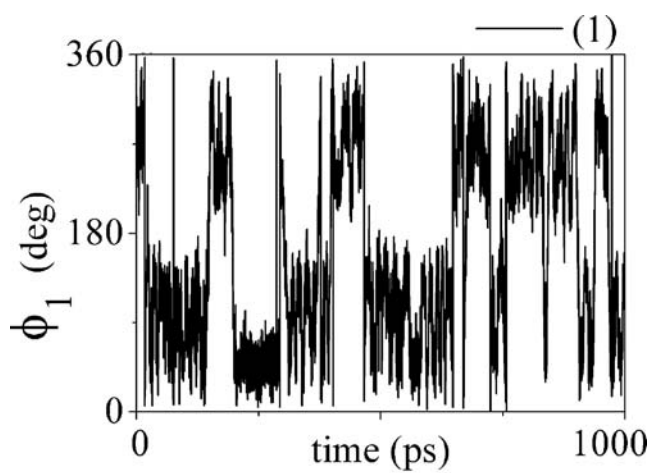
Fig. 5 Trajectories of the torsion angle ϕ_1 for the isolated molecules of the systems at 300 K

Fig. 6 Trajectories of the torsion angle ϕ_1 for a molecule in the cluster environment of the systems at 300 K
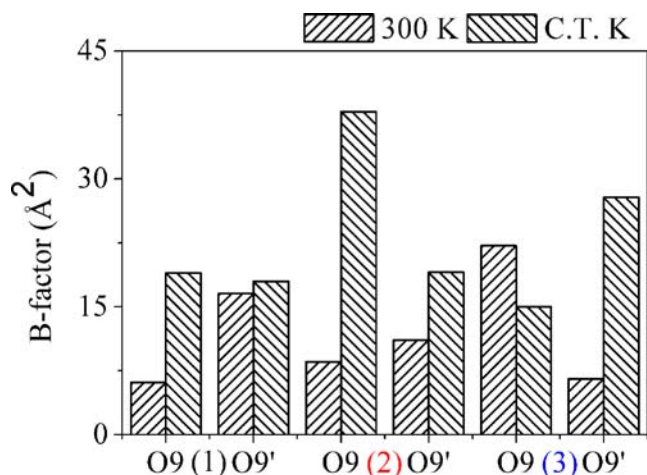
Fig. 7 B-factor values of the carbonyl oxygen atoms for a molecule in the cluster environment of the systems at 300 K and at the clearing temperature (for numbering of the atoms, see Fig. 1)

comparable both at 300 K and the clearing temperature and are therefore not illustrated.

Bending angles and molecular lengths

The bending angle (γ) is a key factor in banana-shaped compounds. Therefore, γ was calculated for single molecules in vacuum and in the environment of the other molecules in clusters with 64 monomers both at 300 K and at the clearing temperature to study aggregation and temperature effects. Within the MD procedure the full width at half maximum (FWHM) and the bending angle of maximal frequency (γ_{max}) were calculated. The results are summarised in Table 3.

Under vacuum, the bending angles of the systems show the sequence γ_{max} (2)>γ_{max} (3)>γ_{max} (1), both at 300 K and at the clearing temperatures. The γ_{max} values show a different trend than the bending angle γ in the most stable structures of the DFT calculation (Table 2). In the case of MD studies, contributions of less favoured conformers are included. In the cluster environment the γ_{max} values at 300 K and at the clearing temperature differ remarkably. Generally, the γ_{max} values of the molecules in the clusters are larger than in vacuum. This can be explained by the

larger conformational degree of freedom of an isolated molecule in the gas phase, which results in conformers with small bending angles also being realised. In the cluster environment, the γ_{max} values of substituted compounds show a different trend at 300 K [γ_{max}(3)>γ_{max}(2)] and at the clearing temperature [γ_{max}(2)>γ_{max}(3)]. A clear increase in the bending angle γ_{max} can be seen going from the single molecule to the cluster aggregation, especially for the dichloro- substituted compound (2) . This tendency is in agreement with experimental results. NMR studies performed in the liquid crystalline state of several bent-core mesogens have proved that the attachment of chlorine atoms at positions 4 and 6 of the central phenyl ring increases the real bending angle up to 165° [14]. The core (L_C) and total (L_T) length of the molecules were calculated as mean values from their trajectories within the MD run. The results are given in Table 4.

The core length (L_C) was defined as the distance between oxygen atoms of the hexyloxy chains. The L_C values show that no significant effect is related either to the temperature or to the aggregation state. The data of the total length (L_T)—distance between the terminal carbon atoms of the hexyloxy chains—indicate an aggregation effect. Molecules in cluster environment have larger L_T values than those in vacuum. This can be attributed to a smaller rate of conformations with folded hexyloxy chains in the aggregated state. The substituted compounds (2) and (3) indicate a different temperature dependence of the L_C and L_T values of the molecules in clusters. This behaviour is in agreement with the tendency found in the bending angle γ_{max} for the molecules in clusters at 300 K and at the clearing temperature (Table 3). The findings of the substituted systems, both in the molecular length and the bending angle of the molecules in the clusters, are hints for their different mesogenic properties.

Radial atom pair distribution function and orientational correlation function

The structure formation of molecules in the clusters can be analysed by calculation of the radial atom pair distribution

Table 3 Full width at half maximum (FWHM) values and bending angles of maximal frequency (γ_{max}) for the systems

System	Single molecule in vacuum				Single molecule in cluster environment			
	300 K		CT		300 K		CT	
	FWHM[a]	γ_{max}	FWHM	γ_{max}	FWHM	γ_{max}	FWHM	γ_{max}
(1)	35	116	30	118	9	120	13	125
(2)	25	121	31	120	9	127	17	140
(3)	22	119	26	119	6	140	12	124

[a] FWHM and γ_{max} values in degrees

Table 4 Molecular lengths of the systems in Å at 300 K and at the clearing temperature

System	Core length (L_C)				Total length (L_T)			
	Single molecule in vacuum		Single molecule in cluster		Single molecule in vacuum			Single molecule in cluster
	300 K	CT	300 K	CT	300 K	CT	300 K	CT
(1)	18.0	22.4	26.7	27.5	18.2	26.4	35.1	36.4
(2)	26.8	26.5	27.8	29.0	35.1	33.6	37.8	38.0
(3)	26.0	25.8	29.3	25.9	33.1	32.7	39.2	34.7

function g(r). The g(r) values were related to the reference atom C2, which describes the position of the central unit of the banana-shaped molecules. The results for the clusters at two different temperatures are illustrated in the Fig. 8. The systems show nearly the same tendency in structure formation both at 300 K and the clearing temperature with the sequence (3)>(1)>(2). Especially in the case of the nitro substituted compound (3), a certain long-range order of molecules can be suggested at both temperatures. The unsubstituted compound (1) shows a short range order only at 300 K, which is decreased at higher temperature. The g(r) curves are comparable for system (2) at both temperatures and indicate a low order.

Further information on the orientation of the molecules results from calculation of the orientational correlation function g(o). The g(o) data are obtained by calculation of the radial dependence of the cosines between the vectors related to the C2 and C5 atoms of the central unit. The
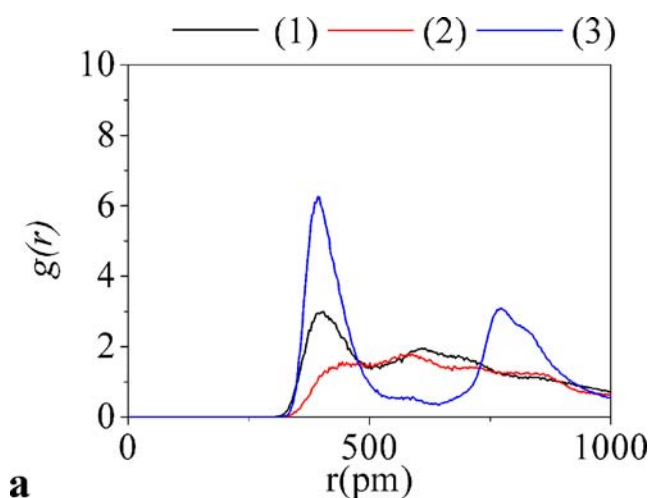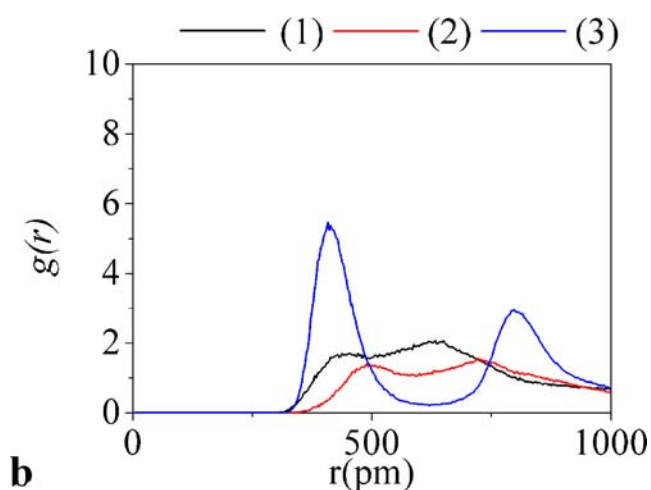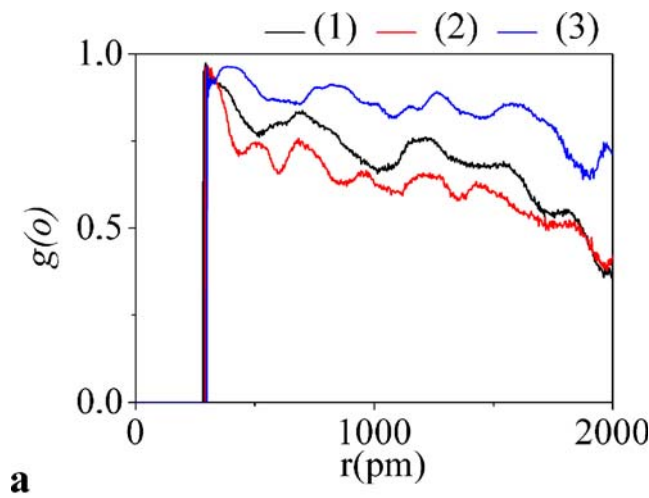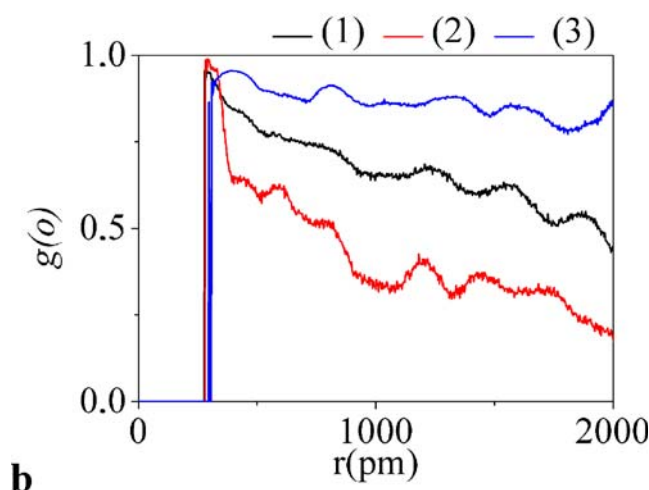

Fig. 8 Radial atom pair distribution functions g(r) for the systems. **a** 300 K, **b** clearing temperature

Fig. 9 Orientational correlation function g(o) for the systems. **a** 300 K, **b** clearing temperature

Table 5 Diffusion coefficients (D) of the clusters at 300 K and at the clearing temperature

System	D (300 K) /10^{-12} m^2 s^{-1}	D (CT) /10^{-12} m^2 s^{-1}
(1)	17.13	51.48
(2)	10.38	23.95
(3)	6.35	173.88

averaging procedure is carried out via the numbers of monomers and of time steps during the MD run. The results are presented in Fig. 9.

The g(o) curves support the trends found in the g(r) results. The long-range order is increased in system *(3)* and reduced in system *(2)*. The effect is more distinct in the curves at the clearing temperature. This is good evidence that chlorination in positions 4 and 6 of the central 1,3-phenylene unit [system *(2)*] can induce significant perturbations in the bent conformations of the monomers, and therefore essentially influence the aggregation of banana-shaped molecules.

Diffusion coefficients and root mean square deviations

The mobility of the molecules in the clusters was investigated by diffusion coefficients calculated using the Einstein model within the MD run [45, 49]. From the averaged mean square displacement (MSD) of the centre of mass, $<\Delta r^2> = 6Dt$, the diffusion coefficient, D, can be obtained by a linear fit. The D values for the systems were calculated from MD runs at 300 K and at the clearing temperature. For both temperatures, the last 500 ps of the equilibration step were considered for comparison, which corresponds to total simulation periods of 1,160–1,660 ps (300 K) and 2,220–2,720 ps (clearing temperature), respectively. The D values are summarised in Table 5.

As expected, the diffusion coefficients are generally larger at higher temperature. Nevertheless, it is remarkable that the D values show different sequences at 300 K [*(1)*>*(2)*>*(3)*] and at the clearing temperature [*(3)*>*(1)*>*(2)*]. This effect cannot be explained by the small differences in the clearing temperatures of the systems, see Table 1. Obviously, the chlorine- and nitro-substituted compounds show a contrary temperature dependence of D related to the unsubstituted species, which again hints at their different aggregation behaviour.

The flexibility of molecules, or parts thereof, in clusters can be indicated by calculation of the root mean square deviations (RMSD) of the corresponding atoms within the MD simulation. The RMSD values of the core and a
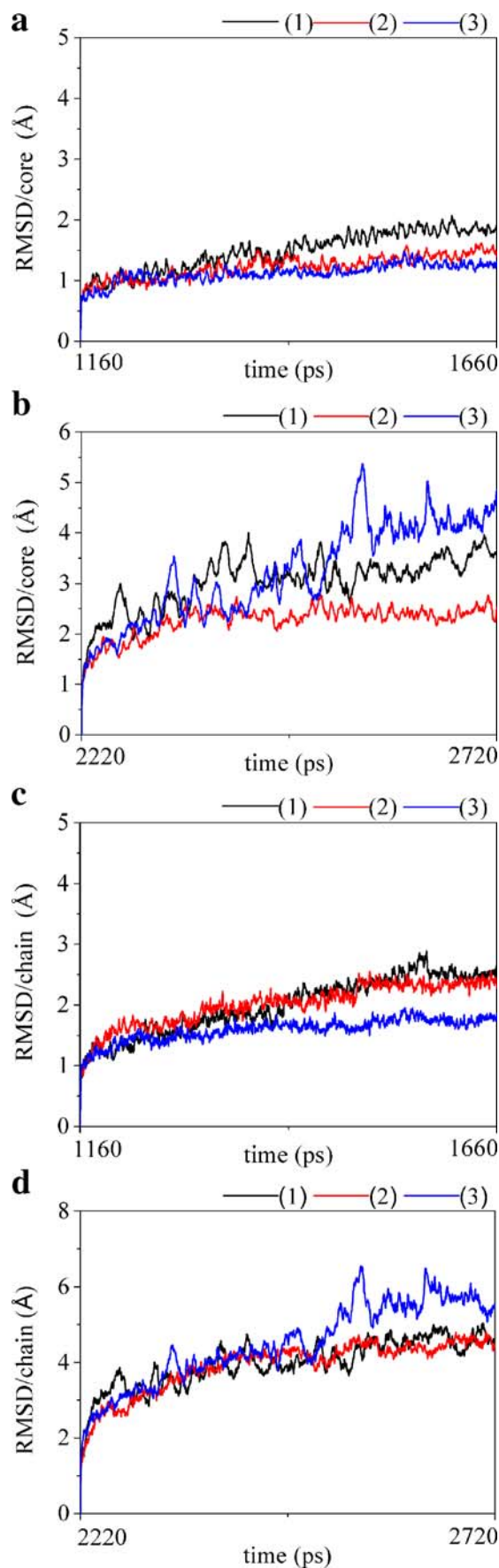
Fig. 10 Root mean square deviation (RMSD) values of the core and the terminal hexyloxy chain for the systems. **a** core/300 K, **b** core/clearing temperature, **c** chain/300 K, **d** chain/clearing temperature

terminal hexyloxy chains were calculated for the three systems to investigate the flexibility of the different segments of the banana-shaped molecules in the aggregated state. In both cases, only the heavy atoms of the segments were considered. The results of MD simulations at 300 K and at the clearing temperature are illustrated in Fig. 10. Similar to the calculation of the diffusion coefficients, the last 500 ps of the MD run were used as the scoring period for the RMSD data.

The curves indicate a significant temperature effect concerning the flexibility of the core and the terminal hexyloxy chain. Generally, the RMSD values are larger at the higher temperature. It is remarkable that the nitro-substituted system (3) shows a higher flexibility at the clearing temperature both in the core and the terminal chains in comparison to the chlorinated compound (2). These findings support the trend found in the calculated diffusion coefficients and are further hints for the different aggregation and mesophase behaviour of the substituted banana-shaped compounds.

Conclusions

Comparative DFT calculations on the B3LYP/6-31G(d) level and MD calculations have been performed on substituted banana-shaped compounds including isolated molecules as well as clusters with up to 64 monomers. DFT studies on isolated molecules indicated that substitution of a nitro group [system (3)] and two chlorine atoms [system (2)] on the central 1,3-phenylene unit of a five-ring system causes significant changes in the structural and polar properties of the molecules. This was illustrated by systematic investigations of relaxed rotational barriers, dipole moments, polarisabilities, bending angles, molecular lengths and electrostatic potential group charges. It is remarkable that the substituted molecules (2) and (3) show different, but mostly opposite, effects in the latter properties in comparison to the unsubstituted compound (1). MD-simulations on isolated molecules essentially support the conformational findings from DFT calculations. Moreover, the temperature effect was studied by simulations both at 300 K and at the clearing temperature of the mesogens. It can be concluded from the trajectories of significant torsion angles, molecular lengths and bending angles that the compounds show a significant aggregation effect related to the substitutents on the central unit. In particular, the radial atom pair distribution functions and orientational correlation functions predict a certain long-range order for the nitro-substituted compound (3), which supports its mesophase properties. The calculations of the diffusion coefficients and RMSDs at 300 K and at the clearing

temperature indicate a remarkable temperature effect, which differs for systems (2) and (3). Despite the limited simulation time and size of the clusters, the findings of MD studies on the atomic level give several hints that will aid our understanding of the different mesophase behaviour of substituted banana-shaped compounds.

References

1. Niori T, Sekine T, Watanabe J, Furukawa T, Takezoe H (1996) J Mater Chem 6:1231–1233
2. Link DR, Natale G, Shao R, Maclennan JE, Clark NA, Korblova E, Walba DM (1997) Science 278:1924–1927
3. Pelzl G, Diele S, Weissflog W (1999) Adv Mater 11:707–724
4. Reddy RA, Tschierske C (2005) J Mater Chem 15:907–961
5. Ros MB, Serrano JL, de la Fuente MR, Folcia CL (2005) J Mater Chem 15:5093–5098
6. Takezoe H, Takanishi Y (2006) Jpn J Appl Phys 45:597–625
7. Reddy RA, Sadashiva BK (2000) Liq Cryst 27:1613–1623
8. Bedel JP, Rouillon JC, Marcerou JP, Laguerre M, Nguyen HT, Achard MF (2000) Liq Cryst 27:1411–1421
9. Weissflog W, Nadasi H, Dunemann U, Pelzl G, Diele S, Eremin A, Kresse H (2001) J Mater Chem 11:2748–2758
10. Reddy RA, Sadashiva BK (2003) Liq Cryst 30:1031–1050
11. Nadasi H, Weissflog W, Eremin A, Pelzl G, Diele S, Das B, Grande S (2002) J Mater Chem 12:1316–1324
12. Shreenivasa Murthy HN, Sadashiva BK (2002) Liq Cryst 29:1223–1234
13. Coleman DA et al (2003) Science 301:1204–1211
14. Eremin A, Nadasi H, Pelzl G, Diele S, Kresse H, Weissflog W, Grande S (2004) Phys Chem Chem Phys 6:1290–1298
15. Heppke G, Parghi D, Sawade H (2000) Ferroelectrics 243:269–276
16. Imase T, Kawauchi S, Watanabe J (2001) J Mol Struct 560:275–281
17. Fodor-Csorba K, Vajda A, Galli G, Jakli A, Demus D, Holly S, Gacs-Baitz E (2002) Macromol Chem Phys 203:1556–1563
18. Ronald YD, Foder-Csorba K, Xu J, Domenici V, Prampolini G, Veracini CA (2004) J Phys Chem B 108:7694–7701
19. Domenici V, Madsen LA, Choi EJ, Samulski ET, Veracini CA (2005) Chem Phys Lett 402:318–323
20. Cacelli I, Prampolini G (2005) Chem Phys 314:283–290
21. Ananda Rama Krishnan S, Weissflog W, Friedemann R (2005) Liq Cryst 7:847–856
22. Weissflog W, Naumann G, Kosata B, Schroder MW, Eremin A, Diele S, Kresse H, Friedemann R, Ananda Rama Krishnan S, Pelzl G (2005) J Mater Chem 15:4328–4337
23. Ananda Rama Krishnan S, Weissflog W, Pelzl G, Diele S, Kresse H, Vakhovskaya Z, Friedemann R (2006) Phys Chem Chem Phys 8:1170–1177
24. Neal MP, Parker AP, Care C (1997) Mol Phys 91:603–624
25. Camp PJ, Allen MP, Masters AJ (1999) J Chem Phys 111:9871–9881
26. Billeter JL, Pelcovits RA (2000) Liq Cryst 27:1151–1160
27. Xu J, Selinger RLB, Selinger JV, Shashidhar R (2001) J Chem Phys 115:4333–4338
28. Memmer R (2002) Liq Cryst 29:483–496

29. Maiti PK, Lansac Y, Glaser MA, Clark NA (2002) Phys Rev Lett 88:065504-1–065504-4
30. Lubensky TC, Radzihovsky L (2002) Phys Rev E 66:031704-1-031704-27
31. Johnston SJ, Low RJ, Neal MP (2002) Phys Rev E 66:061702-1-061702-14
32. Lansac Y, Maiti PK, Clark NA (2003) Phys Rev E 67:011703-1-011703-6
33. Dewar A, Camp PJ (2005) J Chem Phys 123:174907-1–174907-12
34. Orlandi S, Berardi R, Steltzer J, Zannoni C (2006) J Chem Phys 124:124907-1–124907-9
35. Duff N, Wang J, Mann EK, Lacks DJ (2006) Langmuir 22: 9082–9085
36. van Gunsteren WF, Berendsen HJC (1999) Angew Chem Int Ed 29:992–1023
37. Care CM, Cleaver CJ (2005) Rep Prog Phys 68:2665–2700
38. Luckhurst GR (2005) Liq Cryst 32:1335–1364
39. Pleiner H, Brand HR, Cladis PE (2000) Ferroelectrics 243:291–299
40. Frisch MJ, Trucks GW, Schlegel HB, Scuseria GE, Robb MA, Cheeseman JR, Zakrzewski VG, Montgomery JA, Stratman RE, Burant JC, Dapprich S, Millam JM, Daniels AD, Kudin KN, Strain MC, Farkas O, Tomasi J, Barone V, Cossi M, Cammi R, Mennucci B, Pomelli C, Adamo C, Clifford S, Ochterski J, Petersson GA, Ayala PY, Cui Q, Morokuma K, Malick DK, Rabuck AD, Raghavachari K, Foresman JB, Cioslowski J, Ortiz JV, Baboul AG, Stefanov BB, Liu C, Liashenko A, Piskorz P, Komaromi I, Gomperts R, Martin RL, Fox DJ, Keith T, Al-Laham MA, Peng CY, Nanayakkara A, Gonzalez C, Challacombe M, Gill PMW, Johnson BG, Chen W, Wong MW, Andres JL, Gonzales C, Head-Gordon M, Replogle ES, Pople JA (1998) Gaussian 98. Gaussian, Pittsburgh PA
41. Case DA, Pearlman DA, Caldwell JW, Cheatham TE, Wang J, Ross WS, Simmerling CL, Darden TA, Merz KM, Stanton RV, Cheng AL, Vincent JJ, Crowley M, Tsui V, Gohlke H, Radmer RJ, Duan Y, Pitera J, Massova I, Seibel GL, Singh UC, Weiner PK, Kollman PA (2002) AMBER 7. University of California, San Francisco
42. Case DA, Cheatham TE, Darden T, Gohlke H, Luo R, Merz JR KM, Onufriev A, Simmerling C, Wang B, Woods RJ (2005) J Comput Chem 26:1668–1688
43. Jakalian A, Bush BL, Jack DB, Bayly CL (2000) J Comput Chem 21:132–146
44. Ryckaert JP, Ciccotti G, Berendsen HJC (1977) J Comput Phys 23:327–341
45. Friedemann R, Naumann S, Brickmann J (2001) Phys Chem Chem Phys 3:4195–4199
46. Monecke P, Friedemann R, Naumann S, Csuk R (1998) J Mol Model 4:395–404
47. Brooks CL, Karplus M, Pettitt BM (1998) Proteins: a theoretical perspective of dynamics, structures and thermodynamics; advances in chemical physics LXXI, Wiley, New York, pp 192–193
48. Kirkwood JG (1939) J Chem Phys 7:919–925
49. Allen MP, Tildesley DJ (1987) Computer simulations of liquids, Clarendon Press, Oxford, chapter 8
50. Hess S, Frenkel D, Allen MP (1991) Mol Phys 74:765–774
51. Smith SW, Hall CK, Freeman BD (1995) J Chem Phys 102: 1057–1073
52. Bedel JP, Rouillon JC, Marcerou JP, Laguerre M, Nguyen HT, Achard MF (2002) J Mater Chem 12:2214–2220
53. Toriumi H, Samulski ET (1984) In: Griffin AC, Johnson JF (eds) Ordered fluids and liquid crystals, vol 4. Plenum Press New York, London, pp 597–613